

DOI: 10.1002/adma.200700819

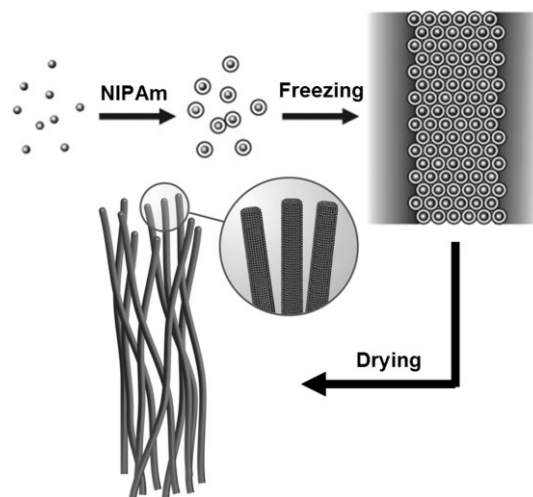
Ice-Templating of Core/Shell Microgel Fibers through ‘Bricks-and-Mortar’ Assembly**

By Qihui Shi, Zesheng An, Chia-Kuang Tsung, Hongjun Liang, Nanfeng Zheng, Craig J. Hawker, and Galen D. Stucky*

Nanoparticles with unique catalytic, electronic, magnetic, optical and optoelectronic properties^[1] provide functional building blocks for organization into spatially well-defined assemblies, allowing for the possible extension of desirable properties of these nanoscale entities to the macroscopic level and the realization of complex devices. In the past decade, ‘bricks-and-mortar’ assembly strategies based on non-covalent interactions have been shown to be successful for the controlled assembly of nanoscale objects into various composite materials.^[2–5] Nanoparticle building blocks bearing molecular recognition elements in their surface monolayer can be readily incorporated into macroscopic assemblies via assembly with a suitable mediator of complementary functionality (e.g., DNA,^[3] nanoparticles,^[4] polymers^[5]). However, a general challenge of the above nanoscale ‘bricks-and-mortar’ approaches is their ability to selectively define morphology at a larger length scale.^[6] For example, the irregular morphology of the aggregates can limit their applications in complex devices. In this Communication, we report a sub-micrometer scale ‘bricks-and-mortar’ assembly approach to create fibers with alternating organic-inorganic arrangement through a simple ice-templating strategy. The fibers are constructed by closely packed monodisperse inorganic nanoparticle (INP)@poly(*N*-isopropylacrylamide) (PNIPAm) core/shell microgels. The well-defined core/shell structure of the particles is critical in the formation of ‘bricks-and-mortar’ fibers: the INP cores are bricks while the mortar is made out of PNIPAm layer on the INPs which serves as an organic glue to hold the bricks together.

Synthetic methods using ice crystals as templates have attracted considerable attention because the ice-templating method is a highly biocompatible, economical and environmentally benign method for the generation of highly pure ma-

terials with unique structures.^[7–11] In pioneering studies, Mahler and Bechtold observed that unidirectional freezing of aqueous silicic acid can produce silica fibers with polygonal cross-sections, a mixture of flakes and honeycombs, or ribbed flakes.^[7] More recently, a directional freezing approach has been used in combination with sol-gel chemistry to produce inorganic fibers,^[8] aligned porous inorganic structures,^[9] aligned porous structures of polymers and polymer/inorganic nanoparticle composites.^[10] In the process of directional freezing, the unidirectional submission of hydrosols, hydrogels or aqueous slurries of metal oxides or polymers to liquid nitrogen induces rapid ice formation (hexagonal form) that exhibits strong anisotropic growth kinetics. Hexagonal ice crystals expel the solutes, which are originally homogeneously dispersed in the aqueous gel, from the forming ice phase and entrap them within the directed channels between the ice crystals.^[12] Therefore, ice crystals grown in the form of platelets with very high aspect ratios can provide a novel template to microscopically define fibers.^[7,8,13] In Scheme 1, we show the assembly of PNIPAm and INP@PNIPAm core/shell microgels into one-dimensional fibrous structures through a convenient freezing method. The produced rounded fibers are on the micrometer scale in diameter and can be as long as several millimeters. Given that polymeric and inorganic fibers with diameters in the range of several micrometers down to tens of nanometers are of considerable interest for various applications,^[13] we believe that the



Scheme 1. A schematic representation of fabrication of core/shell microgel fibers through (Bricks-and-Mortar) assembly.

[*] Prof. G. D. Stucky, Prof. C. J. Hawker, Q. Shi, Dr. Z. An, C.-K. Tsung, Dr. H. Liang
Department of Chemistry and Biochemistry
Materials Research Laboratory, University of California
Santa Barbara, CA 93106 (USA)
E-mail: stucky@chem.ucsb.edu

[**] This work made use of MRL Central Facilities supported by the MRSEC Program of the National Science Foundation under award No. DMR05-20415. QS and HL acknowledge financial support from the UC Discovery Grant program and Genecor International. CKT acknowledges financial support from the National Science Foundation under Award No. DMR 02-33728. ZA acknowledges financial support from the Mitsubishi Chemical Center for Advanced Materials. Supporting Information is available online from Wiley InterScience or from the author.

approach developed here is technologically important because it can be extended to the simple preparation of multifunctional composite fibers in a process that enables the integration of different microgels and nanoparticles that have different individual and, after formation of the composite fiber, different collective functionalities. In order to demonstrate the versatility of this approach, monodisperse silica nanoparticles, core/shell nanoparticles ($\text{SiO}_2@ZrO_2$, $\text{SiO}_2@TiO_2$ and superparamagnetic $\text{Fe}_2O_3@SiO_2$) and hollow nanoparticles (ZrO_2 and TiO_2) were prepared and assembled into fibers through the 'mortar' (PNIPAm)-assisted ice-templating approach.

PNIPAm microgels are materials that exhibit volume phase transitions in response to external stimuli such as temperature, pH, ionic strength, electric field, and antibody-antigen interactions.^[14] The synthesis of PNIPAm microgels crosslinked with *N,N'*-methylenebisacrylamide (BIS) was carried out by conventional precipitation polymerization.^[15] The crosslinker density was tuned to control the size and swelling ratio of the prepared microgels. The silica@PNIPAm core/shell microgels were prepared in a three-step procedure. The silica nanoparticles were prepared according to a modified Stöber synthesis,^[16] and the particle surfaces were then functionalized with the coupling agent methacryloxypropyltrimethoxysilane (MPS)^[17] to allow for growth of a PNIPAm shell.^[18] Two crosslinker densities (5% and 10%) and two sizes of silica nanoparticles (250 nm and 70 nm) were used in the preparation of the silica@PNIPAm core/shell microgels. The microgel samples are denoted as Pa-Sb, where 'a' represents the crosslinker density (%) in the PNIPAm shell and 'b' represents the diameter (nm) of silica nanoparticle core. For example, sample P5-S250 represents the silica@PNIPAm core/shell microgels with 250 nm silica nanoparticles as cores and 5% crosslinking in PNIPAm shell.

The prepared microgels were characterized by scanning electron microscopy (SEM), transmission electron microscopy (TEM) and dynamic light-scattering (DLS). Figure 1 shows the SEM micrographs of the P5-S0 PNIPAm microgels, 250 nm silica nanoparticles after surface modification, P5-S250 and P10-P250 silica@PNIPAm core/shell microgels, respectively. All the samples were separated from aqueous solution by centrifugation and dried in air for SEM imaging. As shown in Figure 1A, PNIPAm microgels are hexagonally packed to form a continuous film, indicating that the microgels are highly monodisperse in size. The silica nanoparticles functionalized with MPS used as the inorganic cores are also monodisperse (PDI 0.01) with a diameter of ~250 nm as measured by SEM with smooth surface (Fig. 1B). For the silica@PNIPAm core/shell microgels, suc-

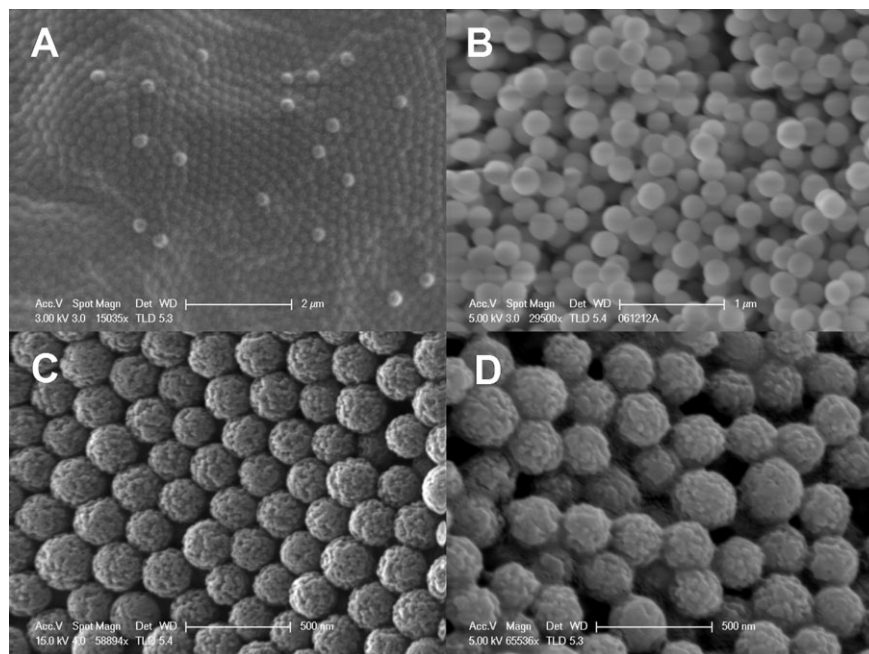


Figure 1. SEM images of A) P5-S0, B) 250 nm silica nanoparticles, C) P5-S250, D) P10-S250. Scale bars: A) 2 μm, B) 1 μm, C,D) 500 nm.

cessful addition of the polymer shells is evidenced by TEM, SEM and DLS characterization. TEM micrographs (Figure 1S, Supporting Information) clearly show a core-shell structure with ~250 nm core and ~50 nm polymeric shell. In SEM images (Fig. 1C,D) the surface morphology of the silica@PNIPAm microgels is more porous and rough than that of the silica particles. Increasing crosslinking density in the shell results in a more dense shell and less porous and less rough surface. DLS was used to measure the average hydrodynamic diameter of the PNIPAm and silica@PNIPAm core/shell microgels as a function of temperature. As shown in Figure 2S, a clear temperature-dependent swelling behavior is observed from the silica@PNIPAm microgels, demonstrating the successful coating of thermosensitive PNIPAm on the silica nanoparticles.

Scheme 1 shows the preparation route of microgel fibers. All microgels were dispersed in water and diluted to 1 wt% aqueous solution, followed by freezing in a -80 °C bath. The ice was then sublimed by freeze-drying and a PNIPAm microgel or silica@PNIPAm scaffold with interweaved fiber bundles was produced (Fig. 2). The scaffold replicated the container in which it was formed (Figure 3S), indicating the control of the macroscopic morphology. The produced material density was found to be about 5 mg/cm³, which is comparable to that of a silica aerogel. SEM micrographs (Fig. 3) of the PNIPAm microgel fibers indicated that the fibers are composed of hexagonally packed PNIPAm microgels and the fibers are rounded, randomly orientated and interweaved. The fibers have a constant diameter along the entire length of the fibers in the range of 1-5 μm and the length varies from hundreds of micrometers to several millimeters. The cross-section image

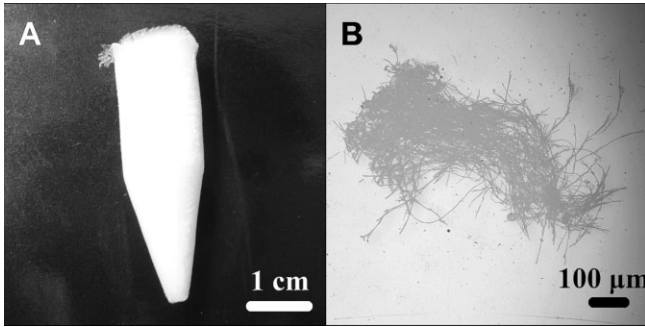


Figure 2. A) Digital image of the P5-S0 microgel scaffold; B) optical microscopy image of a bundle of P5-S0 microgel fibers.

(Fig. 3C) shows that the fibers are not hollow; instead, the insides of the fibers are also composed of closely packed microgels. The ends of the PNIPAM microgel fibers are closed by tapered packing of the microgels (Fig. 3D). PNIPAM microgels are known to be fully hydrated and swollen to their maximum size around 1.5°C ^[18b]. During the freezing process, the microgels are expelled from the forming ice crystals and closely packed into fibrous structures by templating from the high-aspect-ratio ice crystals. In the freeze-drying process, the microgels are dehydrated and hydrogen bonds are formed between the amide groups of the PNIPAM;^[19] therefore, it is possible that the neighboring microgels can be “glued” together by the entanglement and the hydrogen bonding between the pendent chains, leading to stable fibrous structures after freeze-drying. In this way, PNIPAM shells serve as ‘mortar’ to hold the inorganic ‘bricks’ together. The initial concen-

tration of the microgel solution was found to be crucial for the morphology control, as freezing a more concentrated microgel solution results in a mixture of fibers and flakes.

As shown in Figure 4, the silica@PNIPAM P5-S250 microgels also form well-defined fibers, which possess a clear “bricks and mortar” arrangement with the silica nanoparticles representing the bricks and the PNIPAM representing the mortar which joins together the nanoparticle ‘bricks’. The P5-S70 core/shell microgel fibers show a similar morphology and possess a similar arrangement of organic and inorganic elements (Figure 4S) but with smaller periodicity. In addition to the majority of fibers, a small amount of other morphologies were also observed, including branched fibers and elliptical aggregates (Fig. 5S). The P10-S250 microgel fibers shown in Figure 6S have a less regular arrangement of the hybrid microgels, which can be attributed to the increased density of the crosslinker in the PNIPAM shell leading to a more rigid shell structure and fewer/short pendent surface polymer chains. It is known that the mechanical properties of composite materials are significantly determined by the interactions at the interface.^[20] In the microgel-assembled fibers, the interactions between microgels are the entanglement and the hydrogen bonding between the pendent chains of the neighboring microgels. Such interactions integrate the microgels together and make the fibers mechanically strong enough for manipulation. Although the interactions are not very strong in our case, the interfacial bonding can be strengthened by using post-crosslinking comonomers that can covalently crosslink the neighboring microgels, and thus impart more mechanical strength and toughness to the fibers.

Control experiments were also carried out by freezing the aqueous solution of colloidal silica spheres without PNIPAM coating at different solution concentrations. After freeze-drying, the obtained products are powders mainly containing flakes as well as a small amount of spherical aggregates,^[21] further demonstrating the critical role of the PNIPAM layers as ‘mortar’ in the assembling process. Calcination of the hybrid fibers at 550°C in air removed the polymer phase from the organic-inorganic composite. After calcination, the fibers were found to break into shorter rods and silica nanoparticles within the rods were apparently arranged in a much looser way due to the removal of the organic ‘mortar’ (Fig. 7S). Moreover, fibers obtained by freezing a mixture of P5-S70 and P5-S250 microgels in 1:1 ratio have a constant diameter along the whole length (Fig. 8S). Although the two sized microgels are arranged irregularly, they can still closely pack into regular fibers, illustrating the templating effect of ice crystals and the versatility of the approach to assemble different PNIPAM-

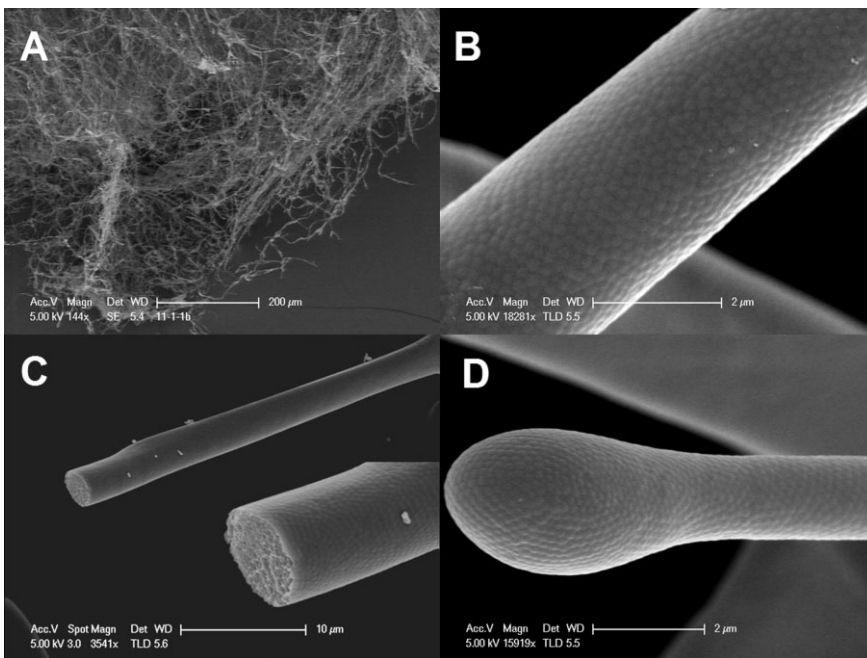


Figure 3. SEM images of P5-S0 microgel fibers. Scale bars: A) 200 μm , B) 2 μm , C) 10 μm , D) 2 μm .

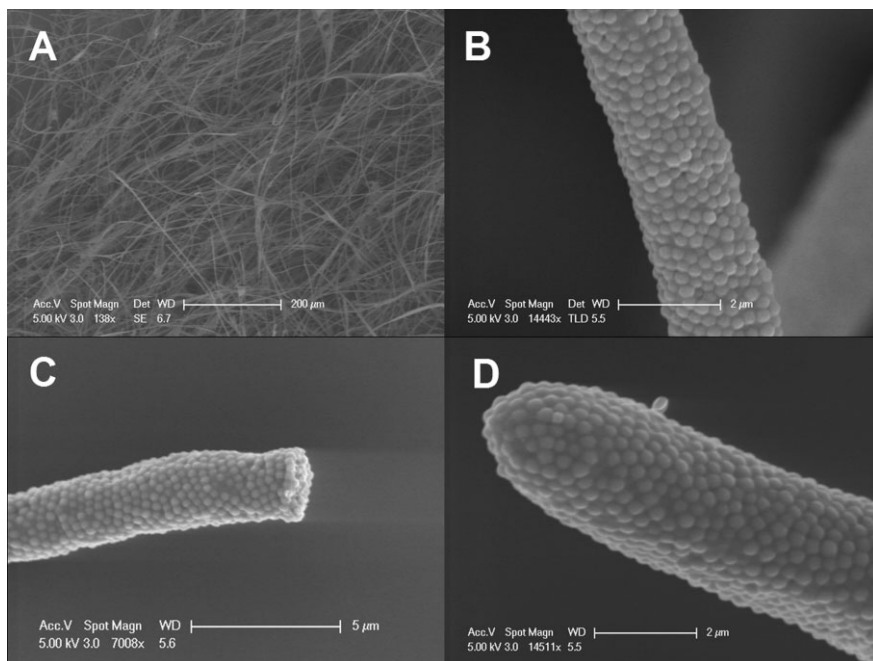


Figure 4. SEM images of P5-S250 microgel fibers. Scale bars: A) 200 μm , B) 2 μm , C) 5 μm , D) 2 μm .

coated particles. It is reasonable to expect that by controlling the local number ratio of the two components (n_A/n_B) and the ratio of the radii of the two components (r_A/r_B), superlattice structures may be achieved.

In the hybrid core/shell microgels, a constant layer of polymer ‘mortar’ is deposited on the surface of the monodisperse inorganic ‘bricks’, representing a highly integrated ‘brick-with-mortar’ structure at the submicron scale for further assembling into organized architectures. The polymer ‘mortar’ plays a critical role in forming ordered organic-inorganic arrangement within the fibers. Such alternating organic-inorganic arrangement is structurally comparable to Deville et al.’s layered hydroxyapatite/epoxy structure^[9c] obtained by a two-step ice-templating approach and Boal’s et al.’s spherical gold nanoparticle/polymer aggregates^[5] based on molecular recognition in a nanoscale ‘bricks-and-mortar’ assembly. Our method is, however, different from the ice-templating-based polymer scaffold processing route reported by Zhang et al.,^[10] in which an aqueous solution containing water-soluble polymer poly(vinylalcohol) (PVA) and 15 nm silica particles was directionally frozen to form an aligned porous polymer/inorganic nanoparticle structure. In this composite, silica nanoparticles were randomly embedded in the polymer matrix without well-defined organic-inorganic arrangement. In our method, integrated submicron ‘brick-with-mortar’ elements are formed before assembly, leading to a highly ordered inorganic-organic alternating structures.

The use of the INP@polymer heterogeneous nanostructure enables a broad spectrum for the manipulation of the composition and properties of the resultant composite fibers. It is ex-

pected that this approach can be extended, in terms of the inorganic core, to various metal nanoparticles,^[22] semiconductor or metal oxide nanoparticles,^[23] or mesoporous microspheres,^[24] and thus impart the fibers optical, magnetic and/or controlled release properties.

In order to demonstrate this, a series of core/shell ($\text{SiO}_2@\text{ZrO}_2$, $\text{SiO}_2@\text{TiO}_2$, $\gamma\text{-Fe}_2\text{O}_3@\text{SiO}_2$) and hollow (ZrO_2 , TiO_2) nanoparticles were prepared as inorganic ‘bricks’ and assembled into fibers through the ‘mortar’ (PNIPAm)-assisted ice-templating approach. For example, a layer of zirconia was coated on the monodisperse silica core through a zirconium butoxide/Brij 30/water/ethanol system (Figs. 5a and 9S).^[25] After grafting with MPS on the surface, a PNIPAm shell was successfully coated on the $\text{SiO}_2@\text{ZrO}_2$ core/shell nanoparticles (Figure 9S). The resultant heterogeneous $\text{SiO}_2@\text{ZrO}_2$ @PNIPAm microgels were then assembled into fibers through the ice-templating approach (Figure 5b and 10S). The silica core of

the $\text{SiO}_2@\text{ZrO}_2$ @PNIPAm microgels can be removed by a treatment of sodium hydroxide (10 M) at room temperature. The hollow ZrO_2 @PNIPAm structure is clearly observed in Figure 5c and 11S, and assembled fibers are shown in Figure 5d. Likewise, titania can be coated on the silica nanoparticles and achieve similar composite fibers and hollow fibers (Fig. 12S). Another example is the superparamagnetic fibers which were assembled from monodisperse superparamagnetic $\gamma\text{-Fe}_2\text{O}_3@\text{SiO}_2$ core/shell nanoparticles derived in a water-in-cyclohexane reverse microemulsion system (Fig. 5e).^[26] A bundle of superparamagnetic fibers shows quick response to a magnet, as shown in Figure 6d. In addition, the polymeric shell can also be conveniently tailored taking advantage of the versatility of the polymer chemistry. For example, various surface functionalities can be incorporated into the polymer shells^[27a] to make bioconjugates and achieve tailored biodegradability. Metallic and semiconductor nanoparticles can also be easily embedded in the polymer network^[27b,c] and thus impart the fibers more functionality. For example, Ag nanoparticles were formed and embedded in PNIPAm shells by reducing silver nitrate with sodium borohydride (Fig. 14S) making use of the ability of PNIPAm to stabilize Ag nanoparticles^[27b]. An absorption peak was observed at about 405 nm (Fig. 14S), which was attributed to the surface plasma wave resonance of silver nanoparticles.^[28]

In summary, fibers with ordered brick-and-mortar arrangement of inorganic phase and organic phase constructed by INP@PNIPAm core/shell microgels have been successfully prepared in a simple ice-templating approach. It is a step-by-step bottom-up approach with control of compositions and

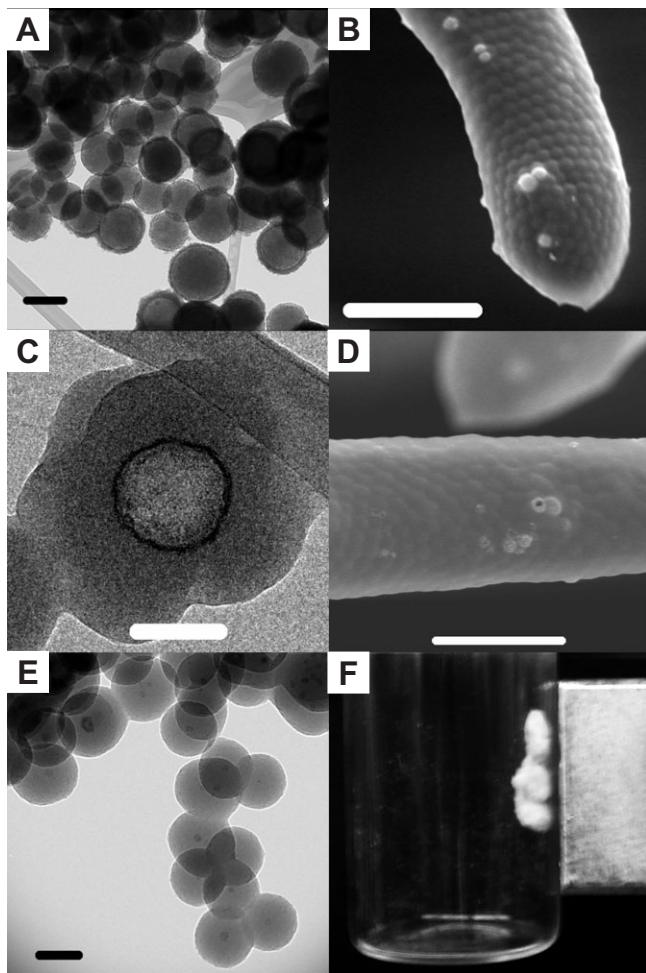


Figure 5. A) TEM image of $\text{ZrO}_2@SiO_2$ nanoparticles; (B) SEM image of $\text{ZrO}_2@SiO_2@PNIPAm$ fibers; (C) TEM image of hollow $\text{ZrO}_2@PNIPAm$ microgels; (D) SEM image of hollow $\text{ZrO}_2@PNIPAm$ fibers; (E) TEM image of $\gamma\text{-Fe}_2\text{O}_3@SiO_2$ nanoparticles; (F) digital image of a bundle of fibers responding to a magnet. Scale bars: A) 200 nm; B) 2 μm ; C) 200 nm; D) 2 μm . E) 50 nm.

architectures at multiple length scales and interfaces. This approach is therefore applicable to different inorganic@organic core/shell building blocks and opens new avenues to the rational functional design of novel materials with well-defined inorganic-organic architectures.

Experimental

Brief Experimental Procedures: 1) The silica nanoparticles were synthesized by the well-known Stöber procedure [16]. 2) To functionalize the silica particles, the desired amount of the alkaline nanoparticle dispersion was directly mixed with methacryloxypropyltrimethoxysilane (MPS) at room temperature [17]. The amount of MPS was calculated to obtain a surface density of 1 molecule per 0.4 nm^{-2} . 3) The core/shell microgel synthesis was carried out by a conventional emulsion polymerization, as described elsewhere [18b]. 4) The microgels were dispersed in water and diluted to 1 wt % aqueous solution, followed by freezing in a $-80\text{ }^\circ\text{C}$ bath. Afterwards, the ice was sublimed by freeze drying, such that a microgel scaffold which consisted

of interweaved fiber bundles was produced. Please find further details in the Supporting Information.

Received: April 5, 2007

Revised: July 31, 2007

- [1] G. Schmid, M. Baumle, M. Geerkens, I. Heim, C. Osemann, T. Sawitowski, *Chem. Soc. Rev.* **1999**, *28*, 179.
- [2] a) J.-M. Lehn, in *Supramolecular Chemistry*, Wiley-VCH, Weinheim, Germany **1995**. b) M. C. T. Fyfe, J. F. Stoddart, *Acc. Chem. Res.* **1997**, *30*, 393. c) S. I. Stupp, V. LeBonheur, K. Walker, L. S. Li, K. E. Huggins, M. Keser, A. Amstutz, *Science* **1997**, *276*, 384.
- [3] a) C. A. Mirkin, R. L. Letsinger, R. C. Mucic, J. J. Storhoff, *Nature* **1996**, *382*, 607. b) A. P. Alivisatos, K. P. Johnsson, X. G. Peng, T. E. Wilson, C. J. Loweth, M. P. Bruchez, P. G. Schultz, *Nature* **1996**, *382*, 609. c) T. A. Taton, R. C. Mucic, C. A. Mirkin, R. L. Letsinger, *J. Am. Chem. Soc.* **2000**, *122*, 6305.
- [4] T. H. Galow, A. K. Boal, V. M. Rotello, *Adv. Mater.* **2000**, *8*, 576.
- [5] A. K. Boal, F. Ilhan, J. E. DeRouche, T. Thurn-Albrecht, T. P. Russell, V. M. Rotello, *Nature* **2000**, *404*, 746.
- [6] G. M. Whitesides, B. Grzybowski, *Science* **2002**, *295*, 2418.
- [7] W. Mahler, M. F. Bechtold, *Nature* **1980**, *285*, 27.
- [8] S. R. Mukai, H. Nishihara, S. Shichi, H. Tamon, *Chem. Mater.* **2004**, *16*, 4987.
- [9] a) S. R. Mukai, H. Nishihara, H. Tamon, *Chem. Commun.* **2004**, 874. b) M. C. Gutierrez, M. Jobbagy, N. Rapun, M. L. Ferrer, F. del Monte, *Adv. Mater.* **2006**, *18*, 1137. c) S. Deville, E. Saiz, R. K. Nalla, A. P. Tomsia, *Science* **2006**, *311*, 515.
- [10] H. F. Zhang, I. Hussain, M. Brust, M. F. Butler, S. P. Rannard, A. I. Cooper, *Nat. Mater.* **2005**, *4*, 787.
- [11] a) S. V. Madhally, H. W. T. Matthew, *Biomaterials* **1999**, *20*, 1133. b) H. -W. Kang, Y. Tabata, Y. Ikada, *Biomaterials* **1999**, *20*, 1339.
- [12] H. Ishiguro, B. Rubinsky, *Cryobiology* **1994**, *31*, 483.
- [13] a) D. Li, Y. Xia, *Adv. Mater.* **2004**, *16*, 1151. b) X.-Y. Sun, R. Shankar, H. G. Börner, T. K. Ghosh, R. J. Spontak, *Adv. Mater.* **2007**, *19*, 87.
- [14] a) T. Miyata, N. Asami, T. Uragami, *Nature* **1999**, *399*, 766. b) R. Pelton, *Adv. Colloid Interface Sci.* **2000**, *85*, 1. c) S. Nayak, L. A. Lyon, *Angew. Chem. Int. Ed.* **2005**, *44*, 7686.
- [15] W. McPhee, K. C. Tam, R. Pelton, *J. Colloid Interface Sci.* **1993**, *156*, 24.
- [16] W. Stöber, A. Fink, E. Bohn, *J. Colloid Interface Sci.* **1968**, *26*, 62.
- [17] E. Bourgeat-Lami, J. Lang, *J. Colloid Interface Sci.* **1999**, *210*, 281.
- [18] a) L. S. Zha, Y. Zhang, W. L. Yang, S. K. Fu, *Adv. Mater.* **2002**, *14*, 1090. b) M. Karg, I. Pastoriza-Santos, L. M. Liz-Marzan, T. Hellweg, *ChemPhysChem* **2006**, *7*, 2298.
- [19] Y. Ono, T. Shikata, *J. Am. Chem. Soc.* **2006**, *128*, 10030.
- [20] H. J. Gao, B. H. Ji, I. L. Jager, E. Arzt, P. Fratzl, *Proc. Natl. Acad. Sci. USA* **2003**, *100*, 5597.
- [21] S. Hyuk, O. O. Park, *Appl. Phys. Lett.* **2002**, *22*, 4133.
- [22] a) N. Zheng, J. Fan, G. D. Stucky, *J. Am. Chem. Soc.* **2006**, *128*, 6550. b) C.-K. Tsung, X. S. Kou, Q. H. Shi, J. P. Zhang, M. H. Yeung, J. F. Wang, G. D. Stucky, *J. Am. Chem. Soc.* **2006**, *128*, 5352.
- [23] S. T. Selvan, T. T. Tan, J. Y. Ying, *Adv. Mater.* **2005**, *17*, 1620.
- [24] a) Y. Han, J. Y. Ying, *Angew. Chem. Int. Ed.* **2005**, *44*, 288. b) T. A. Ostomel, Q. H. Shi, C. -K. Tsung, H. J. Liang, G. D. Stucky, *Small* **2006**, *2*, 1261.
- [25] P. M. Arnal, C. Weidenthaler, F. Schuth, *Chem. Mater.* **2006**, *18*, 2733.
- [26] a) D. K. Yi, S. T. Selvan, S. S. Lee, G. C. Papaefthymicu, D. Kundaliya, J. Y. Ying, *J. Am. Chem. Soc.* **2005**, *127*, 4990. b) D. K. Yi, S. S. Lee, G. C. Papaefthymicu, J. Y. Ying, *Chem. Mater.* **2006**, *18*, 614.
- [27] a) Z. S. An, W. Tang, C. J. Hawker, G. D. Stucky, *J. Am. Chem. Soc.* **2006**, *128*, 15054. b) Y. Lu, Y. Mei, M. Drechsler, M. Ballauff, *Angew. Chem. Int. Ed.* **2006**, *45*, 813. c) C. L. Bai, Y. Fang, Y. Zhang, B. B. Chen, *Langmuir* **2004**, *20*, 263.
- [28] F. Mafune, J. Y. Kohno, Y. Takeda, T. Kondow, *J. Phys. Chem.* **2000**, *104*, 9111.